Research Article

Realization of Colored Multicrystalline Silicon Solar Cells with SiO$_2$/SiN$_x$:H Double Layer Antireflection Coatings

Minghua Li,[1] Libin Zeng,[1] Yifeng Chen,[1,2] Lin Zhuang,[1] Xuemeng Wang,[3] and Hui Shen[1,3]

[1] *Institute for Solar Energy Systems, Guangdong Provincial Key Laboratory of Photovoltaic Technologies,*
  State Key Laboratory of Optoelectronic Materials and Technologies, Sun Yat-sen University, Guangzhou 510006, China
[2] *State Key Lab of PV Science and Technology, Trina Solar, Changzhou 213031, China*
[3] *Shunde SYSU Institute for Solar Energy, Shunde 528300, China*

Correspondence should be addressed to Hui Shen; drshenhui@gmail.com

We presented a method to use SiO$_2$/SiN$_x$:H double layer antireflection coatings (DARC) on acid textures to fabricate colored multicrystalline silicon (mc-Si) solar cells. Firstly, we modeled the perceived colors and short-circuit current density (J_{sc}) as a function of SiN$_x$:H thickness for single layer SiN$_x$:H, and as a function of SiO$_2$ thickness for the case of SiO$_2$/SiN$_x$:H (DARC) with fixed SiN$_x$:H (refractive index n = 2.1 at 633 nm, and thickness = 80 nm). The simulation results show that it is possible to achieve various colors by adjusting the thickness of SiO$_2$ to avoid significant optical losses. Therefore, we carried out the experiments by using electron beam (e-beam) evaporation to deposit a layer of SiO$_2$ over the standard SiN$_x$:H for 156 × 156 mm^2 mc-Si solar cells which were fabricated by a conventional process. Semisphere reflectivity over 300 nm to 1100 nm and *I-V* measurements were performed for grey yellow, purple, deep blue, and green cells. The efficiency of colored SiO$_2$/SiN$_x$:H DARC cells is comparable to that of standard SiN$_x$:H light blue cells, which shows the potential of colored cells in industrial applications.

1. Introduction

With the rapid development of photovoltaic (PV) industry, the decorative performance of solar modules gradually becomes an important issue, for instance, in building-integrated photovoltaics (BIPV) systems [1–3]. For industrial mass production multicrystalline silicon (mc-Si) solar cells, the front surface is usually covered by a layer of SiN$_x$:H deposited by plasma-enhanced chemical vapor deposition (PECVD), which serves for both passivation and antireflection [4]. When the thickness and refractive index of the SiN$_x$:H are optimized, the colors of solar cells look light blue. To realize colored solar cells, Tobias et al. reported a method by changing the thickness of the silicon nitride (n = 1.9) or zinc sulfide (n = 2.3), which acts as a single antireflection coating (ARC) on random pyramid textures [5]. However, this method results in significant J_{sc} losses. To improve the optical performance, multilayer ARC had been studied by simulation and experiments on polished surface [6, 7]. For pyramid texture surface, we have showed that it is possible for DARC colored cells to achieve equal J_{sc} to standard blue cell [8]. For acid texture, simulations and experiments on 3 × 3 cm^2 mc-Si cells are under progress in our group [9]. Nevertheless, experimental reports on colored full dimensional industrial mc-Si cells with acid textures are still absent.

In this paper, we present our recent progress on simulations and experiments to fabricate colored mc-Si solar cells with a dimension of 156 × 156 mm^2. In this study, we focus on using SiO$_2$/SiN$_x$:H DARC to replace the single SiN$_x$:H layer, and using electron beam (e-beam) evaporation technique to deposit a layer of SiO$_2$ over the standard SiN$_x$:H after the conventional mc-Si cell fabrication. The solar cells with DARC stacks show various colors according to thickness of the SiO$_2$ layer (top layer). Interestingly, the conversion efficiency of colored solar cells shows a little variation (+0.1% to −0.7%) compared to the reference cells with standard single SiN$_x$:H layer.
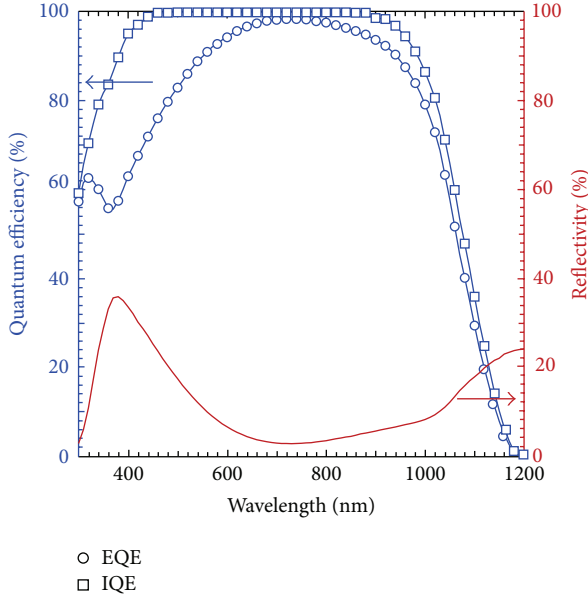
FIGURE 1: The quantum efficiency of solar cell with SiN$_x$:H SARC.

2. Optical Simulation

The typical acidic textured morphology of multicrystalline silicon is concave-like texture. We have simulated the morphology as three-dimensional ellipsoid by Monte Carlo ray tracing method [10], so we employed this model to calculate the reflectivity of the solar cells with both single SiN$_x$:H layer and SiO$_2$/SiN$_x$:H stacks. The simulations of colors are accomplished by calculating the tristimulus values X, Y, and Z using the following equations:

$$X = k \int \text{Flux}(\lambda) R(\lambda) x(\lambda) d\lambda,$$
$$Y = k \int \text{Flux}(\lambda) R(\lambda) y(\lambda) d\lambda, \quad (1)$$
$$Z = k \int \text{Flux}(\lambda) R(\lambda) z(\lambda) d\lambda,$$

where Flux(λ) is the wavelength dependent photon flux under AM 1.5G spectrum; $R(\lambda)$ is the reflectivity; and $x(\lambda)$, $y(\lambda)$, and $z(\lambda)$ are color matching functions defined by the International Commission on Illumination (CIE) [11, 12].

Furthermore, for better evaluation of the optical performance, we calculated the short-circuit current density (J_{sc}) with

$$J_{sc} = \int_{300\,\text{nm}}^{1200\,\text{nm}} q \cdot \text{Flux}(\lambda) \cdot \text{IQE}(\lambda) \cdot [1 - R(\lambda)] d\lambda, \quad (2)$$

where q is the element charge, IQE(λ) the measured internal quantum efficiency of a conventional multicrystalline silicon solar cells (as shown in Figure 1), and $R(\lambda)$ the simulated reflectivity.

Figure 2(a) shows the simulated color and the J_{sc} of multicrystalline silicon solar cells as a function of the thickness of single SiN$_x$:H ARC. As we can see, the peak of J_{sc}

arrives with SiN$_x$:H thickness of 80 nm, but then J_{sc} drops significantly when the thickness deviates from 80 nm. To achieve yellow, purple, and green colors, single ARC will suffer 2~3 mA/cm^2 J_{sc} losses. For comparison, we simulated the case of SiO$_2$/SiN$_x$:H DARC, with the bottom layer fixed to SiN$_x$:H (thickness = 80 nm, n = 2.1) and with the thickness of SiO$_2$ (n = 1.46) varied from 0 nm to 300 nm as the top layer. Note that 0 nm SiO$_2$ means the situation of optimal single layer SiN$_x$:H. As shown in Figure 2(b), a slight boost of J_{sc} can be observed when the SiO$_2$ thickness varies from 0 nm to 150 nm, while the color changes from light blue, to grey yellow, red, and purple. On the other hand, when the SiO$_2$ thickness continues to increase to 300 nm, deep blue and green colors will appear, with a small J_{sc} losses of up to 0.5 mA/cm^2. These indicate that the optical losses can be greatly suppressed with SiO$_2$/SiN$_x$:H DARC, comparing with the single SiN$_x$:H ARC in Figure 2(a).

3. Experiments

To further prove the simulations, experiments were carried out on industrial p-type mc-Si wafers with dimensions of 156 mm × 156 mm, and the wafer resistivity is between 1~3 Ωcm. After acidic texturing and cleaning, a standard POCl$_3$ diffusion is performed in a quartz tube to form an emitter with sheet resistivity of 80 Ω/□. The samples were then coated with a SiN$_x$:H layer in a PECVD (Roth&Rau) system. The deposition of SiN$_x$:H was controlled to hold the refractive index of SiN$_x$:H (n = 2.1) and its thickness of 80 nm. The metallizations are realized by screen printing to form the "H-pattern" front grid and full aluminum rear contact after firing. The I-V measurements were carried out with Berger I-V tester under calibration. To form the SiO$_2$/SiN$_x$:H DARC structure, SiO$_2$ thin films were deposited by electron beam (e-beam) evaporation on the already fabricated solar cells. To avoid the deposition of SiO$_2$ on the front side of the busbars, a steel mask was utilized as the shelter [13]. High purity SiO$_2$ (99.99%) granules were used as the source material for evaporation and the source-to-substrate distance is 50 cm. E-type electron gun was employed for source evaporation. Ion bombardment was used to remove the dust on the substrate surface before deposition. The substrates were preheated and temperature was controlled at 200°C during the process. High purity oxygen (99.99%) was introduced into the chamber to maintain a pressure of 3.0×10^{-2} Pa and used as reactive gas during the deposition. The deposition rate was controlled using a quartz crystal sensor placed near the substrate and was set to 2 Å/s. The deposition time was adjusted to modulate the thicknesses of the SiO$_2$ as the top layer of 84 nm, 136 nm, 190 nm, and 220 nm, respectively. Six samples were fabricated for each thickness. The structure of the solar cell with SiO$_2$/SiN$_x$:H DARC is schematically shown in Figure 3.

The Fourier transformed infrared spectroscopy (FTIR) measurement for the SiO$_2$ thin film has been made at 25°C using a Thermo-Nicolet 6700 FTIR spectrometer. The chemical states of the SiO$_2$ were investigated by X-ray photoelectron spectroscopy (XPS) using an ESCALab250 (U.K) spectrometer with monochromatic Al Kα radiation
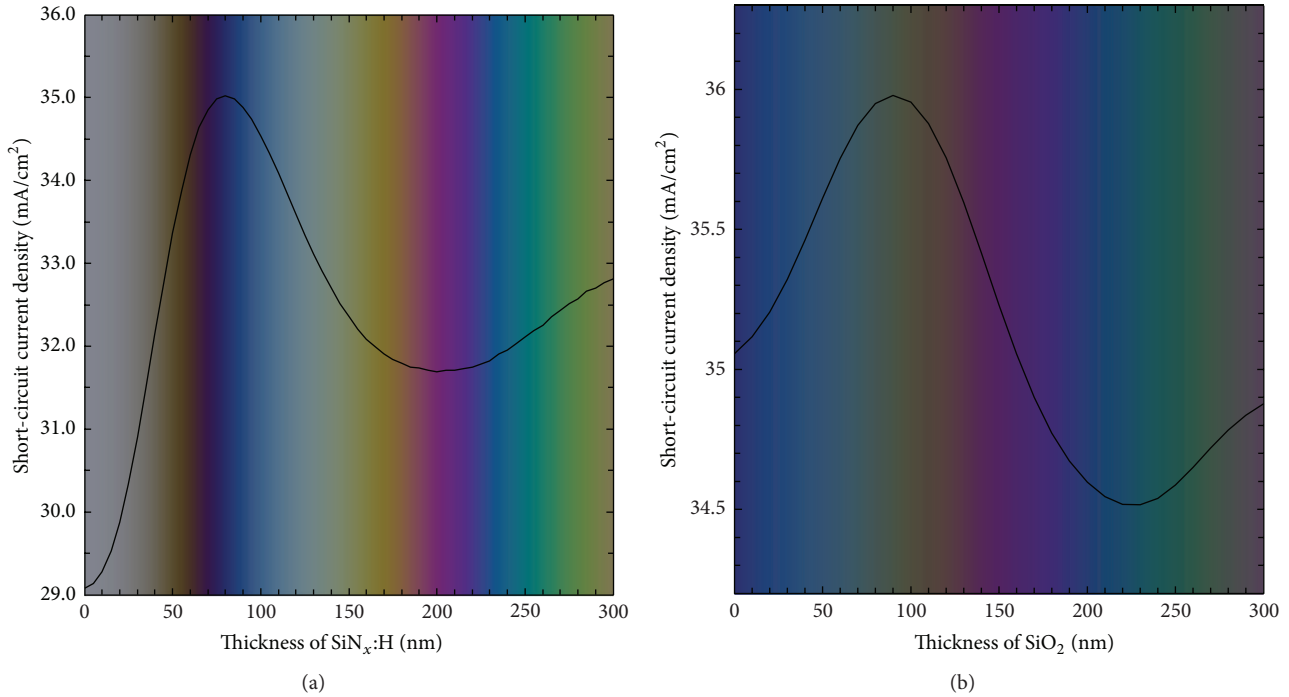
(a)

(b)

FIGURE 2: Calculated perceived color and short-circuit current density as a function of the thickness of (a) the standard single layer SiN_x:H (with $n = 2.1$ at 633 nm) on a concave-like textured solar cell and (b) SiO_2 on top of the standard SiN_x:H ($n = 2.1$ at 633 nm, and thickness = 80 nm).
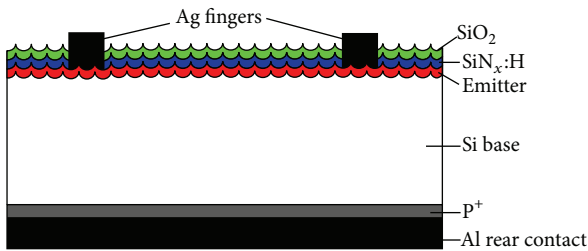

FIGURE 3: Schematic of solar cell with SiO_2/SiN_x:H DARC.

($h\nu = 1486$ eV). All binding energies were calibrated with respect to C 1s spectral line at 284.8 eV. The morphology of the surface was characterized by field emission scanning electron microscope (JEOL, JSM-6330F). The refractive indexes of the SiN_x:H and SiO_2 coatings were measured by a Sentech SE800 ellipsometer. The spectral reflectivity between 300 nm and 1100 nm was measured by a Hitachi U-4100 spectrophotometer. The quantum efficiency (QE) measurements were performed by a solar cell spectral response measurement system (PV measurement, QEX10). Finally, the I-V characteristics of the DARC solar cells were measured using a Berger I-V tester on a solar cell production line.

4. Results and Discussion

4.1. Films Characterization and Potential Stability. In order to get a qualitative spectra of SiO_2 thin film compositions, we have performed Fourier transformed infrared spectroscopy
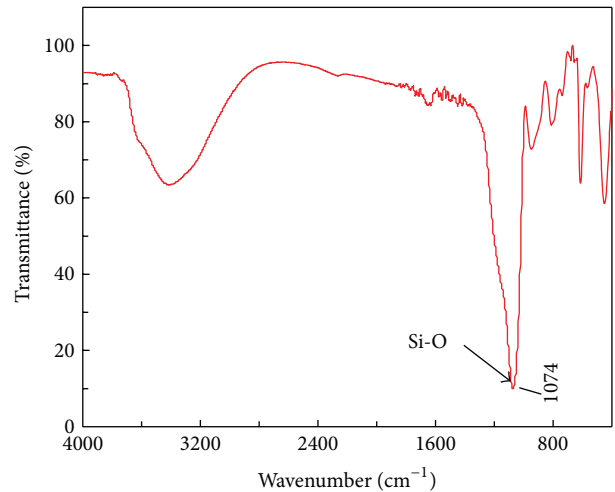
FIGURE 4: FTIR transmittance spectra of SiO_2 thin film.

(FTIR) analysis. The samples were deposited bifacially with the same film thicknesses on the polished silicon wafer. The spectra are presented in Figure 4. The band in the 1040–1150 cm^{-1} range is assigned to the stretching vibration mode Si–O [14, 15]. For the supplement of oxygen during the SiO_2 deposition, a clear Si–O intensity peak (1074 cm^{-1}) is observed for the SiO_2 layer, which is related to the high oxygen content in this layer. The SEM images are shown in Figure 5. A clear concave-like acid texture can be seen

(a)

(b)

FIGURE 5: SEM images of (a) top view and (b) cross-section of multicrystalline silicon solar cell with SiO_2 (190 nm)/SiN_x:H (80 nm) DARC.

(a)

(b)

FIGURE 6: XPS spectra of SiO_2: (a) Si 2p and (b) O 1s.
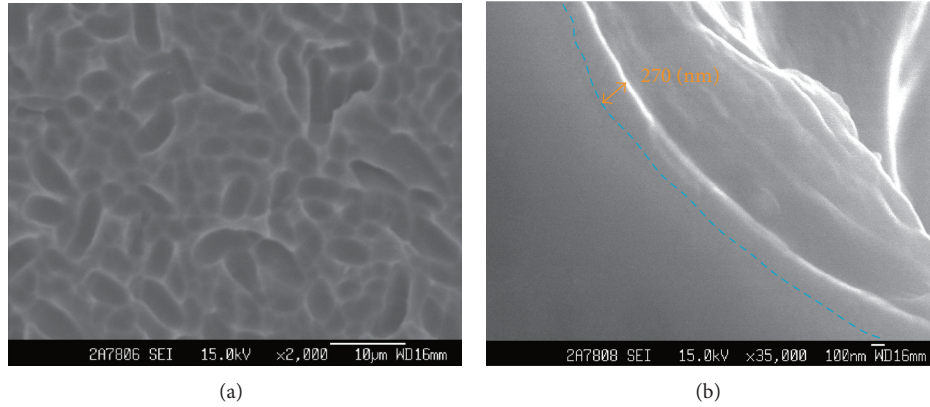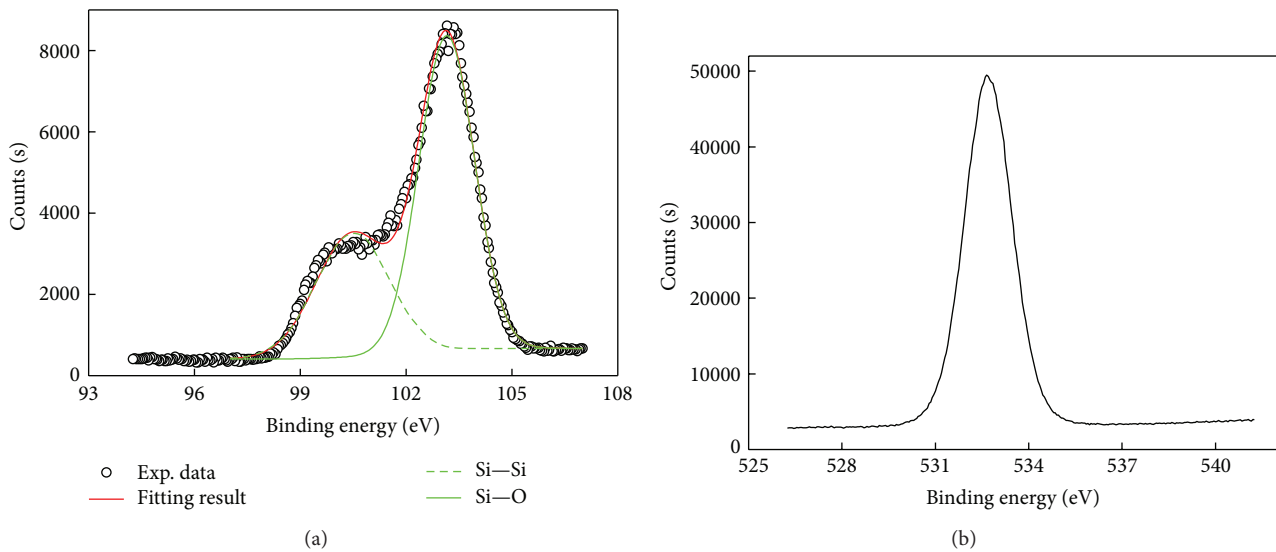
in Figure 5(a), while the interface between silicon and SiO_2/SiN_x:H (deep blue color, with 80 nm SiN_x:H and 190 nm SiO_2) is illustrated in Figure 5(b).

XPS was applied to determine the chemical state of the Si and O elements, which can confirm the presence of SiO_2 layer in DARC. High-resolution spectra are shown in Figure 6(a) for Si 2p and Figure 6(b) for O 1s, respectively. The Si peaks were fitted using Gaussian curves. It is evident that two Si 2p peaks are located at 100.5 eV and 103.2 eV, as seen in Figure 6(a), which can be attributed to the signal of SiO_2. It is recognized that the binding energy of Si 2p related to SiO_2 is dependent on the oxygen composition [16]. Then, the films prepared by electron beam evaporation in this study were nearly stoichiometric silicon dioxide.

It is important that the surface of the solar cell endures various kinds of physical conditions. Structural stability of the antireflection coating is a key issue. SiN_x:H films are widely used in photovoltaic industries due to their strong durability, excellent passivation properties, good dielectric characteristics, and resistance against corrosion by water.

In our work, SiO_2 thin films were deposited on the conventional solar cells with precoated SiN_x:H single layer. The colored cells with SiO_2/SiN_x:H double layer antireflection coating do not need to suffer high temperature treatment again in the subsequent process, including encapsulation. For the SiO_2/SiN_x:H antireflection coating structure, due to different lattice spacing of substrate and silicon nitride layers, as well as stacking faults in the crystal structure, pin holes, or interstitial atoms, tension in deposited SiN_x:H layers can occur, while SiO_2 film exhibits compressing force. The opposite mechanical property can lead to the lower stress in the double layers. In addition, the thermal expansion coefficient of SiO_2 is smaller than that of silicon; thus the interface stress in SiO_2/SiN_x:H is smaller than that of SiN_x:H/SiO_2 [17]. Consequently, such a good interface matching can avoid film cracks at the SiO_2/SiN_x:H interface. Besides, it has been confirmed that the SiN_x:H and SiO_2 films also have good thermal stability [18]. Hence, all the factors shown above are the main reasons why SiO_2 is the best candidate to form double layer antireflection coatings with SiN_x:H. On the other
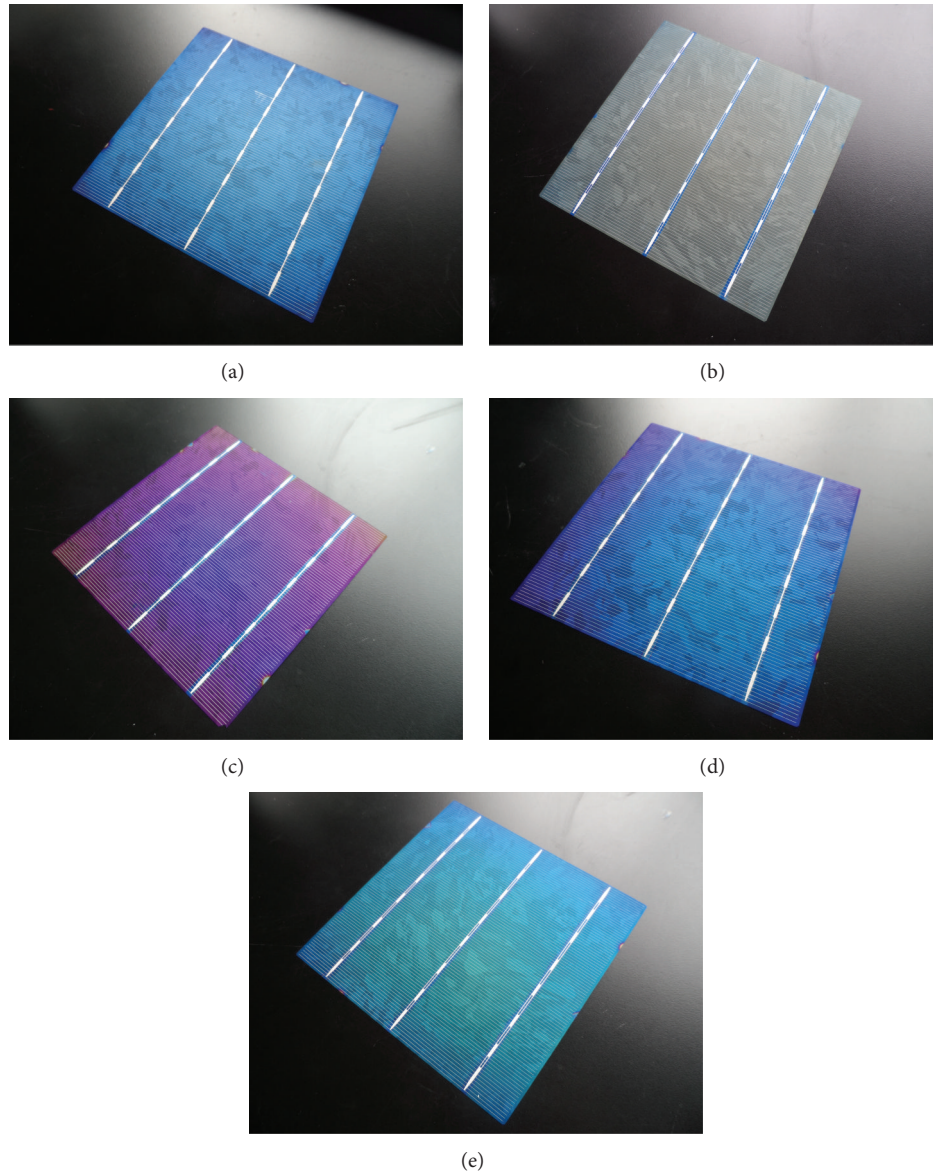
FIGURE 7: Photographs of the colored multicrystalline silicon solar cells with different layer stacks. (a) SiN_x:H (80 nm). (b) SiO_2 (84 nm)/SiN_x:H (80 nm). (c) SiO_2 (136 nm)/SiN_x:H (80 nm). (d) SiO_2 (190 nm)/SiN_x:H (80 nm). (e) SiO_2 (220 nm)/SiN_x:H (80 nm).

hand, for the deposition process of SiO_2 on the conventional solar cells, the films properties are highly dependent upon both deposition parameters and subsequent processing. In order to obtain good thin film adhesion force on the substrate, we established the optimal process parameters to achieve high quality SiO_2 films, which are transparent in the visible range and have less light absorption. The stability of SiO_2 films, SiN_x:H films, and SiO_2/SiN_x:H double films has been well investigated by many groups before [19–21]. For the SiO_2/SiN_x:H double layers, postanneal treatment can not only improve the optical property, but also decrease residual stress. Based on above discussion, we believe the SiO_2/SiN_x:H structure has superior stability, which can be used in the colored solar cells.

4.2. Optical Characterization. Figure 7 presents the photographs of the fabricated DARC mc-Si solar cells (156 mm × 156 mm) samples with SiO_2 thickness equal to 84 nm (grey yellow), 136 nm (purple), 190 nm (deep blue), and 220 nm (green) covering on 80 nm SiN_x:H (light blue). It is apparent that colored cells are achievable by varying the thickness of SiO_2 (top layer) on the solar cell with SiN_x:H (bottom layer). For the whole cells, the color is basically uniform. However, small chromatic aberrations in the edges still can be observed, which indicated that higher spatial uniformity during the deposition is required for further improvements.

Figure 8 depicts the reflectivity of single layer SiN_x:H with optimized thickness of 80 nm, as well as with the reflectivity of SiO_2/SiN_x:H DARC for optimized grey yellow, purple,

TABLE 1: Performances of colored mc-Si cells with SiO_2/SiN_x : H ARC compared to single SiN_x : H cell (measurement conditions: AM 1.5 G, 100 mW/cm², 25°C).

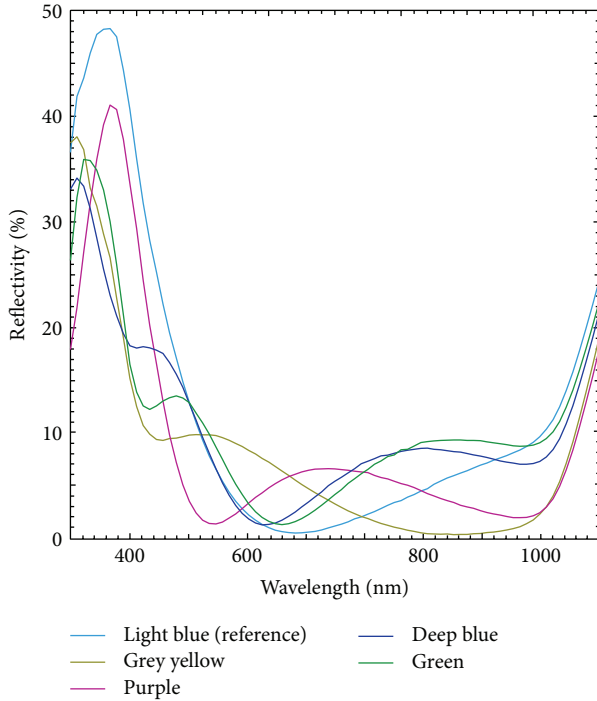| Samples	Color	Eff. (%)	FF (%)	J_{sc} (mA/cm²)	V_{oc} (mV)
SiN_x : H (80 nm) (reference)	Light blue	16.87	76.89	35.18	623.6
SiO_2 (84 nm)/SiN_x : H (80 nm)	Grey yellow	16.97	76.66	35.77	618.6
SiO_2 (136 nm)/SiN_x : H (80 nm)	Purple	16.75	77.07	34.91	622.4
SiO_2 (190 nm)/SiN_x : H (80 nm)	Deep blue	16.13	76.93	33.86	619.2
SiO_2 (220 nm)/SiN_x : H (80 nm)	Green	16.43	77.05	34.30	621.6

FIGURE 8: Reflectivity curves of the single SiN_x:H layer (light blue curve for SiN_x:H 80 nm) and double ARC with SiO_2 thickness of 84 nm (grey yellow curve), 136 nm (purple curve), 190 nm (deep blue curve) and 220 nm (green curve) on top of 80 nm SiN_x:H.

FIGURE 9: Calculated short-circuit current density of the colored solar cell module as a function of the thickness of SiO_2 on top of the standard SiN_x:H (n = 2.1 at 633 nm, and thickness = 80 nm).

deep blue, and green cells. As shown in Figure 8, the hunches of reflectivity move gradually from short wavelength to long wavelength, which explained the color switch by increasing the thickness of SiO_2.

4.3. I-V Characteristics of Colored Solar Cells. All *I-V* parameters presented in the study are averaged with six samples of each group. All measurements were conducted under the standard test conditions (AM 1.5G spectrum, 100 mW/cm², 25°C). Prior to the measurements, the simulator was calibrated with a reference multicrystalline silicon solar cell, which was calibrated by the Fraunhofer ISE. Table 1 summarizes the average performance parameters of colored mc-Si solar cells, compared to the standard light blue cells with 80 nm single SiN_x:H. As shown in Table 1, the FF of each group is nearly the same, while the V_{oc} shows small degradation for colored cells, which probably caused by the surface damages introduced during the e-beam evaporation.

The main power loss of colored cell comes from the J_{sc} losses, which reflects that the optical losses are still the dominating efficiency limit for colored solar cells. However, we demonstrate that comparable cell efficiency of colored solar cell is available, comparing to standard light blue cell, and 16.97% efficiency for grey yellow cell (abs. 0.1% higher than standard cell) with V_{oc} of 618.6 mV, J_{sc} of 35.77 mA/cm², and FF of 76.66% when SiO_2 (84 nm)/SiN_x:H (80 nm) DARC is applied.

4.4. Colored Solar Cell Module Simulation. The matching ARC to refraction index of the cover materials in a module is one of the key factors that ultimately determine the optical properties of PV modules. To investigate the behaviors of solar cells with double layer antireflection coatings after encapsulation, we simulated the module J_{sc} by Monte Carlo ray tracing method. EVA was considered as the encapsulation material in the simulation since currently it is the most widely used with the refractive index of approximately 1.5 at 633 nm. Since the multiple total internal reflections between glass and air were neglected, the J_{sc} was underestimated slightly.

As shown in Figure 9, the J_{sc} is equal to 33.11 mA/cm² when the thickness of SiO_2 is 0 nm, which is the case of single

layer SiN_x:H ARC. As the SiO_2 thickness increases from 0 nm to 50 nm, J_{sc} increases slightly and reaches the maximum value, and then the J_{sc} experienced a slow decrease; it drops to 32.78 mA/cm^2 when the thickness of SiO_2 is 300 nm. In overall, the advantages of DARCs are more limited in modules with EVA than in cells. This is mainly because the glass and EVA have a refractive index which is very close to SiO_2, and EVA has strong absorptivity in short wavelength. Therefore, the suppression of reflectivity in short wavelength via DARCs is not so notable anymore. Better encapsulation materials (such as PVB, silicone resin, and high transmittance glass) are needed to obtain high-performance module for the BIPV [22]. Additionally, the NICE (New Industrial Solar Cell Encapsulation) module concept [23, 24] seems to be a better option. Contrary to standard modules, NICE modules do not use EVA-like encapsulants. The use of nitrogen instead of EVA avoids any UV-cut from the incident spectrum that is typically observed with standard encapsulants. Further researches for this subject are now under investigation to optimize the module conversion efficiency.

5. Conclusions

We have successfully fabricated colored multicrystalline silicon solar cells by depositing an additional layer of SiO_2 via e-beam evaporation on the standard SiN_x:H layer. By controlling the thickness of SiO_2, even better cell performances can be achieved; for example, grey yellow color cells have a higher J_{sc} than reference cells. With SiO_2/SiN_x:H DARC, the following benefits can be achieved.

(1) Various colors can be achieved by adjusting the thickness of SiO_2.

(2) The cells conversion efficiencies are very comparable, which indicates the potential of a smaller mismatch for colorful modules fabricated with cells of different colors.

(3) Small degradations of V_{oc} are found after the deposition of SiO_2, which indicated that only little surface damage is caused by e-beam evaporation.

Therefore, more accurate e-beam evaporation process controls are needed for further works to improve the uniformity and reduce the surface damages. With SiO_2/SiN_x:H DRAC, colored mc-Si solar cells with comparable cell efficiencies are available for industrial applications, for instance, in architectural integration in buildings.
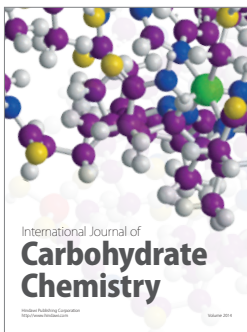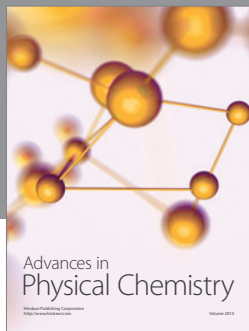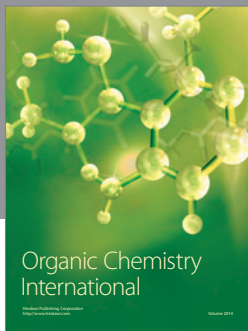
Acknowledgments

References

[1] T. J. N. Schoen, "Building-integrated PV installations in the netherlands: examples and operational experiences," *Solar Energy*, vol. 70, no. 6, pp. 467–477, 2001.

[2] R. Charron and A. K. Athienitis, "Optimization of the performance of double-façades with integrated photovoltaic panels and motorized blinds," *Solar Energy*, vol. 80, no. 5, pp. 482–491, 2006.

[3] C. L. Cheng, C. S. S. Jimenez, and M. C. Lee, "Research of BIPV optimal tilted angle, use of latitude concept for south orientated plans," *Renewable Energy*, vol. 34, no. 6, pp. 1644–1650, 2009.

[4] A. G. Aberle, "Overview on SiN surface passivation of crystalline silicon solar cells," *Solar Energy Materials and Solar Cells*, vol. 65, no. 1, pp. 239–248, 2001.

[5] I. Tobias, A. El Moussaoui, and A. Luque, "Colored solar cells with minimal current mismatch," *IEEE Transactions on Electron Devices*, vol. 46, no. 9, pp. 1858–1865, 1999.

[6] M. Spiegel, G. Willeke, P. Fath et al., "Colored solar cells with single, multiple and continuous layer antireflection coatings," in *Proceedings of the 13th European Photovoltaic Solar Energy Conference*, pp. 417–420, Nice, France, 1995.

[7] J. H. Selj, T. T. Mongstad, R. Søndenå, and E. S. Marstein, "Reduction of optical losses in colored solar cells with multilayer antireflection coatings," *Solar Energy Materials and Solar Cells*, vol. 95, no. 9, pp. 2576–2582, 2011.

[8] Y. F. Chen, P. P. Altermatt, Y. Yang, Z. Q. Feng, and H. Shen, "Color modulation of c-Si solar cells without significant current-loss by means of a double anti-reflective coating (DARC)," in *Proceedings of the 27th European Photovoltaic Solar Energy Conference and Exhibition*, pp. 2014–2016, September 2012.

[9] L. B. Zeng, Y. F. Chen, S. M. Chen et al., "Simulation and fabrication to reduce optical losses in colored multi-crystallinesilicon solar cells using double layer antireflection coatings," In press.

[10] L. B. Zeng, Y. F. Chen, W. J. Ge et al., "Optimization of multilayer antireflection coatings for multicrystalline silicon solar cells," in *Proceedings of the 27th European Photovoltaic Solar Energy Conference and Exhibition*, pp. 1299–1302, September 2012.

[11] The CIE Central Bureau, "Colorimetric observers," ISO/CIE Standard 10527, The CIE Central Bureau, Vienna, Austria.

[12] The CIE Central Bureau, "Colorimetric illuminants," ISO/CIE Standard 10526, The CIE Central Bureau, Vienna, Austria.

[13] H. Shen, Y. Chen, X. Xu et al., A structure to form colorful protective thin film via mask, granted, P.R. China patent, Application No. 201010168604. 9, Publish No. CN101834230A, 2010. 09. 15.

[14] P. V. Bulkin, P. L. Swart, and B. M. Lacquet, "Effect of process parameters on the properties of electron cyclotron resonance plasma deposited silicon-oxynitride," *Journal of Non-Crystalline Solids*, vol. 187, pp. 403–408, 1995.

[15] S. K. Ghosh and T. K. Hatwar, "Preparation and characterization of reactively sputtered silicon nitride thin films," *Thin Solid Films*, vol. 166, pp. 359–366, 1988.

[16] A. Strass, P. Bieringer, W. Hansch et al., "Fabrication and characterisation of thin low-temperature MBE-compatible silicon oxides of different stoichiometry," *Thin Solid Films*, vol. 349, no. 1-2, pp. 135–146, 1999.

[17] J. Camassel and A. Tiberj, "Strain effects in device processing of silicon-on-insulator materials," *Applied Surface Science*, vol. 212-213, pp. 742–748, 2003.

[18] B. Lenkeit, S. Steckemetz, F. Artuso, and R. Hezel, "Excellent thermal stability of remote plasma-enhanced chemical vapour deposited silicon nitride films for the rear of screen-printed bifacial silicon solar cells," *Solar Energy Materials and Solar Cells*, vol. 65, no. 1, pp. 317–323, 2001.

[19] T. Minami, T. Utsubo, T. Yamatani, T. Miyata, and Y. Ohbayashi, "SiO_2 electret thin films prepared by various deposition methods," *Thin Solid Films*, vol. 426, no. 1-2, pp. 47–52, 2003.

[20] A. El Amrani, I. Menous, L. Mahiou, R. Tadjine, A. Touati, and A. Lefgoum, "Silicon nitride film for solar cells," *Renewable Energy*, vol. 33, no. 10, pp. 2289–2293, 2008.

[21] Z. Chen, Z. Lv, and J. Zhang, "PECVD SiO_2/Si_3N_4 double layers electrets on glass substrate," *IEEE Transactions on Dielectrics and Electrical Insulation*, vol. 15, no. 4, pp. 915–919, 2008.

[22] I. Tobías, C. del Cañizo, and J. Alonso, "Chapter 7. Crystalline silicon solar cells and modules," in *Handbook of Photovoltaic Science and Engineering*, p. 293, John Wiley & Sons, New York, NY, USA, 2003.

[23] R. Einhaus, K. Bamberg, R. D. Franclieu et al., "New industrial solar cell encapsulation (NICE) technology for PV module fabrication at drastically reduced costs," in *Proceedings of the 19th European Photovoltaic Solar Energy Conference and Exhibition*, pp. 2371–2374, August 2004.

[24] J. Dupuis, E. Saint-Sernin, O. Nichiporuk et al., "NICE module technology—from the concept to mass production: a 10 years review," in *Proceedings of the 38th IEEE Photovoltaic Specialists Conference*, pp. 3183–3186, Austin, Tex, USA, 2012.

International Journal of
Medicinal Chemistry
Hindawi Publishing Corporation
http://www.hindawi.com
Volume 2014

Organic Chemistry
International
Hindawi Publishing Corporation
http://www.hindawi.com
Volume 2014

International Journal of
Photoenergy
Hindawi Publishing Corporation
http://www.hindawi.com
Volume 2014

International Journal of
Analytical Chemistry
Hindawi Publishing Corporation
http://www.hindawi.com
Volume 2014

Advances in
Physical Chemistry
Hindawi Publishing Corporation
http://www.hindawi.com
Volume 2014

International Journal of
Carbohydrate Chemistry
Hindawi Publishing Corporation
http://www.hindawi.com
Volume 2014

Journal of Quantum Chemistry
Hindawi Publishing Corporation
http://www.hindawi.com
Volume 2014

The Scientific World Journal
Hindawi Publishing Corporation
http://www.hindawi.com
Volume 2014

Hindawi
Submit your manuscripts at
http://www.hindawi.com

Journal of
Analytical Methods in Chemistry
Hindawi Publishing Corporation
http://www.hindawi.com
Volume 2014

Journal of
Spectroscopy
Hindawi Publishing Corporation
http://www.hindawi.com
Volume 2014

International Journal of
Inorganic Chemistry
Hindawi Publishing Corporation
http://www.hindawi.com
Volume 2014

International Journal of
Electrochemistry
Hindawi Publishing Corporation
http://www.hindawi.com
Volume 2014

Journal of
Applied Chemistry
Hindawi Publishing Corporation
http://www.hindawi.com
Volume 2014

Bioinorganic Chemistry and Applications
Hindawi Publishing Corporation
http://www.hindawi.com
Volume 2014

Journal of
Theoretical Chemistry
Hindawi Publishing Corporation
http://www.hindawi.com
Volume 2014

Chromatography Research International
Hindawi Publishing Corporation
http://www.hindawi.com
Volume 2014

Journal of
Catalysts
Hindawi Publishing Corporation
http://www.hindawi.com
Volume 2014

Journal of
Chemistry
Hindawi Publishing Corporation
http://www.hindawi.com
Volume 2014

International Journal of
Spectroscopy
Hindawi Publishing Corporation
http://www.hindawi.com
Volume 2014